Quantitative assessment of non-conservative radiation forces in an optical trap

Giuseppe Pesce[1,3], Giorgio Volpe[2], Anna Chiara De Luca[1,3], Giulia Rusciano[1,3] and Giovanni Volpe[4,5]

[1] *Dipartimento di Scienze Fisiche, Università di Napoli "Federico II", Complesso Universitario Monte S. Angelo, Via Cintia, 80126 Napoli, Italy*
[2] *CNISM - Consorzio Nazionale Interuniversitario per le Scienze Fisiche della Materia - Sede di Napoli*
[3] *ICFO - Institut de Ciencies Fotoniques, Mediterranean Technology Park, 08860, Castelldefels (Barcelona), Spain*
[4] *Max-Planck-Institut für Metallforschung, Heisenbergstr. 3, 70569 Stuttgart, Germany*
[5] *2. Physikalisches Institut, Universitt Stuttgart, Pfaffenwaldring 57, 70550 Stuttgart, Germany*

PACS 87.80.Cc – Optical trapping in biophysical techniques
PACS 82.70.Dd – Colloids
PACS 05.40.Jc – Brownian motion

Abstract. - The forces acting on an optically trapped particle are usually assumed to be conservative. However, the presence of a non-conservative component has recently been demonstrated. Here we propose a technique that permits one to quantify the contribution of such a non-conservative component. This is an extension of a standard calibration technique for optical tweezers and, therefore, can easily become a standard test to verify the conservative optical force assumption. Using this technique we have analyzed optically trapped particles of different size under different trapping conditions. We conclude that the non-conservative effects are effectively negligible and do not affect the standard calibration procedure, unless for extremely low-power trapping, far away from the trapping regimes usually used in experiments.

Introduction. – The detection and measurement of forces and torques in microscopic systems is an important goal in many areas such as biophysics, colloidal physics and hydrodynamics of small systems. Since 1993, the photonic force microscope (PFM) has become a standard tool to probe such forces [1–3]. A typical PFM setup comprises an optical trap – an highly-focused Gaussian light beam – that holds a probe – a dielectric or metallic particle of micrometer size – and a position sensing system. Using a PFM it has been possible to measure forces as small as 25 fN [4] and torques as small as $4000\,\mathrm{fN}\cdot\mathrm{nm}$ [5].

In order to assess the mechanical properties of microscopic systems, the first step is always to have an accurately calibrated optical probe. Modelling the interaction between the light of a focused laser beam and an extended dielectric or metallic object can be a complicated task [6]. The electromagnetic theory is relatively straightforward for the Rayleigh and the geometrical optics regimes [7, 8]. However, most applications of PFM involve particles whose characteristic size is comparable to the wavelength of the light employed. In this case the exact solutions for the force-field are cumbersome to come by. Fortunately there

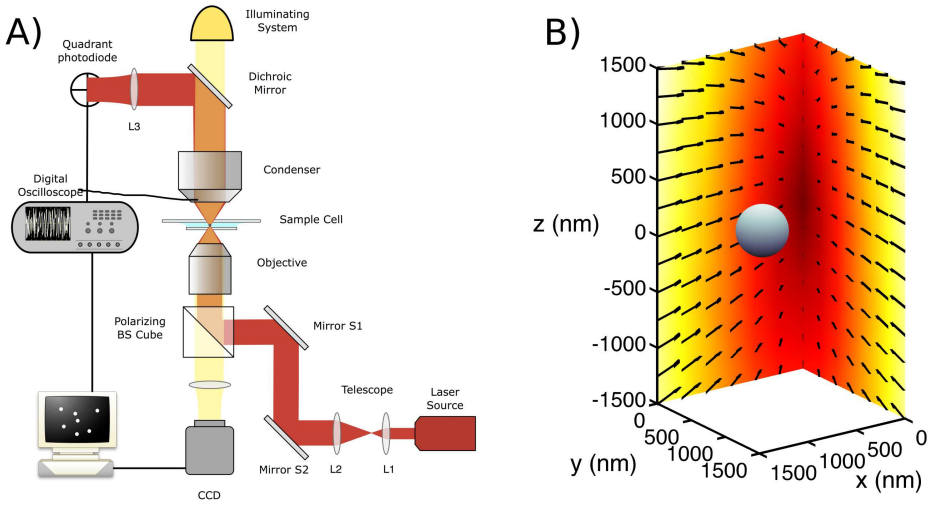

Fig. 1: (A) Schematics of the experimental setup. (B) Forces acting on a colloidal particle held by an optical trap. The lines represent the force-field and the color the modulus of the force. A slight bending of the force lines due to the non-conservative component of the force-field can be observed [see also Fig. 2].

are several straightforward methods to experimentally measure the trap parameters – i.e., the trap stiffness and the conversion factor between voltage and length – and, therefore, the force exerted by the optical tweezers on an object. The most commonly employed methods are the *drag force method*, the *equipartition method*, the *potential analysis method* and the *power spectrum or correlation method* [9]. The latter two [10, 11], in particular, are usually considered the most reliable ones.

An implicit assumption of all these calibration methods is that, for small displacements of the probe from the center of an optical trap, the restoring force is proportional to the displacement. Hence, an optical trap is assumed to act on the probe like a Hookeian spring with a fixed stiffness. This condition implicates that the the force-field produced by the optical forces must be conservative, excluding the possibility of a rotational component. This is actually true to a great extend in the plane perpendicular to the beam propagation direction (e.g., x-y plane in Fig. 1(B)) for a standard optical trap generated by a Gaussian beam. However, this has been shown not to be true in a plane parallel to the beam propagation [8, 12, 13] (e.g., x-z plane in Fig. 1(B)).

Back in 1992 Ashkin already pointed out that, in principle, scattering forces in optical tweezers do not conserve mechanical energy, and that this could have some measurable consequences [8]. In particular, this non-conservative force would produce a dependence of the axial equilibrium position of a trapped micro-sphere as a function of its transverse position in the trapping beam (see Fig. 10(C) of Ref. [8]); such prediction was first confirmed by Merenda and colleagues [12]. Recently Roichman and colleagues [13] have directly investigated the non-conservative component and have discussed the implications that this might have for optical tweezers-based experiments making use of the thermal fluctuations in the calibration procedure.

Here we propose a technique that permits one to evaluate the relative weight of the non-conservative component of the optical forces. It is based on a previous work [11], where it was proposed an enhancement of the PFM to measure force-fields with a non-conservative component. We use this technique to analyze various optically trapped particles in different trapping conditions. The main result is that the non-conservative effects are effectively negligible and do not affect the standard calibration procedure, unless for extremely low-

power trapping, far away from the trapping regimes usually used in experiments.

Theory. – Assuming a very low Reynolds number regime [14, 15], the motion of a Brownian particle in the presence of an optical force-field can be described by the vectorial Langevin equation

$$\dot{\mathbf{r}}(t) = \frac{1}{\gamma}\mathbf{f}(\mathbf{r}(t)) + \sqrt{2D}\mathbf{h}(t), \tag{1}$$

where $\mathbf{r}(t)$ is the probe position and $\mathbf{f}(\mathbf{r})$ is the optical force acting on the particle, which depends on the position of the particle itself, of course since $\mathbf{r}$ is time-dependent then also $\mathbf{f}$ varies over time, $\gamma = 3\pi d\sigma$ is its friction coefficient, d is its diameter, σ is the medium viscosity, $\sqrt{2D}\gamma\mathbf{h}(t)$ is a vector of independent white Gaussian random processes describing the Brownian forces, $D = k_B T/\gamma$ is the diffusion coefficient, T is the absolute temperature, and k_B is the Boltzmann constant.

The system that we are going to characterize is radially symmetric. It is, therefore, easier to study it in cylindrical coordinates. Eq.(1) can be projected in cylindrical coordinates as

$$\begin{cases} \dot{\rho}(t) = \frac{1}{\gamma} f_\rho(\rho,\theta,z) + \sqrt{2D} h_\rho(t) \\ \dot{\theta}(t) = \frac{1}{\gamma\rho(t)} f_\theta(\rho,\theta,z) + \sqrt{2D}\frac{h_\theta(t)}{\rho(t)} \\ \dot{z}(t) = \frac{1}{\gamma} f_z(\rho,\theta,z) + \sqrt{2D} h_z(t) \end{cases} \tag{2}$$

where $h_\rho(t)$, $h_\theta(t)$ and $h_z(t)$ are independent white Gaussian random processes with unitary variance.

Since an optical trap generated by a Gaussian beam is symmetrical, the particle is effectively diffusing freely with respect to the coordinate θ and we can assume that $f_\theta(\rho,\theta,z) = 0$. We can, therefore, study the movement of the particle only with respect to the coordinates r and z. Following a procedure similar to the one in Ref. [11], to which we refer for more details, we can linearize the force-field near the equilibrium position $(\rho_0, z_0) = (0,0)$ and rewrite the Brownian particle equations of motion as

$$\begin{cases} \dot{\rho}(t) = -\frac{k_\rho}{\gamma}\rho(t) + \epsilon\frac{k_\rho}{\gamma} z(t) + \sqrt{2D} h_\rho(t) \\ \dot{z}(t) = -\epsilon\frac{k_\rho}{\gamma}\rho(t) - \eta\frac{k_\rho}{\gamma} z(t) + \sqrt{2D} h_z(t) \end{cases} \tag{3}$$

where k_ρ is the optical trap stiffness in the x-y plane, ηk_ρ is the trap stiffness along the z axis, η is the ratio between the trap stiffness in the x-y plane and the one along z, which is typically ~ 0.1, and ϵ represent the relative contribution of the non-conservative component of the force-field.

The terms $-\frac{k_\rho}{\gamma}\rho(t)$ and $-\eta\frac{k_\rho}{\gamma}z(t)$ represent the elastic restoring forces which are the conservative part of the force-field and the terms $+\epsilon\frac{k_\rho}{\gamma}z(t)$ and $-\epsilon\frac{k_\rho}{\gamma}\rho(t)$ represent the non-conservative part of the field. In Fig. 2(A) an example of such a force-field is drawn. In Fig. 2(B) only the non-conservative component is depicted.

The statistical analysis of the Brownian trajectories permits one to reconstruct the force-field acting on the particle. Here we will use the autocorrelation functions (ACFs) of the radial (ρ) and axial (z) particle position, and the difference between the two cross-correlation functions (DCCF) between the the radial (ρ) and axial (z) particle position.

Assuming $\epsilon << 1$ and $\epsilon << \eta$, the ACFs for ρ and z are decoupled

$$\mathrm{ACF}_\rho(\tau) = \frac{\gamma D}{k_\rho}\exp\left(-\frac{k_\rho}{\gamma}|\tau|\right) \tag{4}$$

and

$$\mathrm{ACF}_z(\tau) = \frac{\gamma D}{\eta k_\rho}\exp\left(-\frac{\eta k_\rho}{\gamma}|\tau|\right). \tag{5}$$

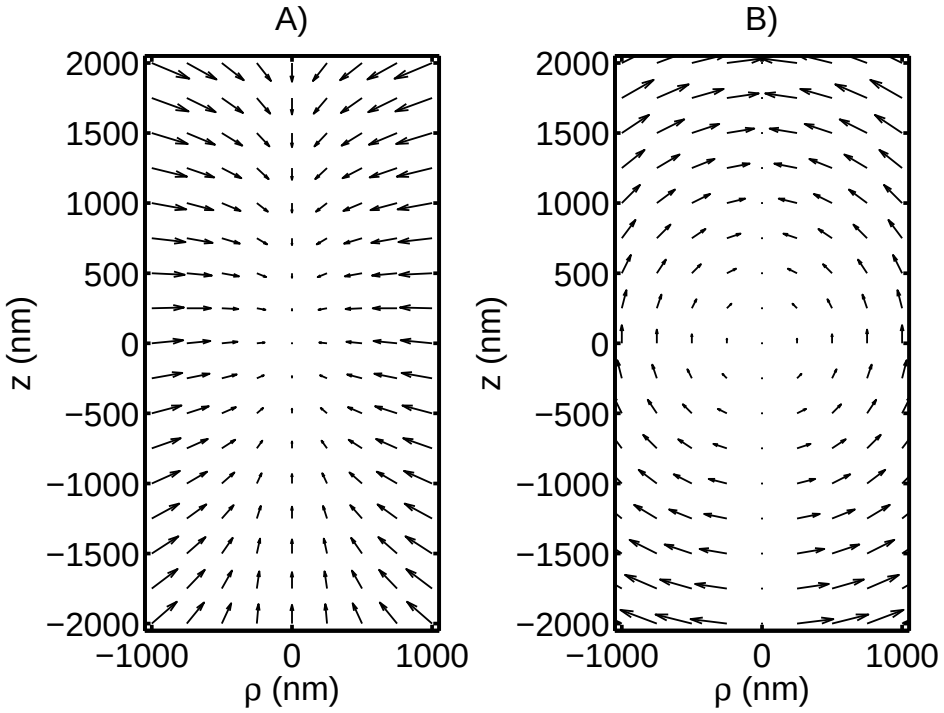

Fig. 2: (A) Force field generated by an optical trap in the presence of a rotational component and (B) the rotational part of the force-field with $\eta = 0.3$ and $\epsilon = 0.1$. Note that these values are larger than typical ones, which are usually about $\eta \sim 0.1$ and $\epsilon \sim 0.05$, in order to have a clearer qualitative picture of the way they affect the force-field.

These expressions are the standard ones for a conservative force-field and are independent from ϵ [11]. The DCCF is

$$\mathrm{DCCF}_{\rho z}(\tau) = 4D\frac{\varepsilon\gamma}{(1+\eta)k_\rho}\exp\left(-\frac{(1+\eta)k_\rho}{2\gamma}\,|\tau|\right)\cdot \\ \cdot\frac{\sinh\left(\frac{k_\rho}{2\gamma}\sqrt{|(1-\eta)^2-4\varepsilon^2|}\tau\right)}{\sqrt{|(1-\eta)^2-4\varepsilon^2|}}. \tag{6}$$

Equations (4), (5) and (6) can be used to fit the values for k_ρ, η, and ϵ, and therefore to reconstruct the force-field up to the first order. In particular, the ACFs (4) and (5) can be used directly to fit the values of k_ρ and η. Once these values are estimated, it is possible to fit the value ϵ by using the slope of the DCCF (6) around $\tau = 0$.

Once the force-field parameters have been fitted, it is possible to calculate the torque acting on the particle due to the presence of the rotational component of the force-field [5,11] as

$$T = \epsilon k_\rho\left[\mathrm{Var}(\rho) + \mathrm{Var(z)}\right], \tag{7}$$

and the circulation rate as

$$\Omega = \epsilon\frac{k_\rho}{2\pi\gamma}. \tag{8}$$

Experimental setup. – The experimental setup, shown in Fig. 1(A), is described in details in Ref. [16]. The PFM comprises a home-made optical microscope with a high-numerical-aperture water-immersion objective lens (Olympus, UPLAPO60XW3, NA=1.2)

and a frequency and amplitude stabilized Nd-YAG laser ($\lambda = 1.064\,\mu$m, 500 mW maximum output power, Innolight Mephisto).

Polystyrene micro-spheres (Serva Electrophoresis, 1.06g/cm^3 density, 1.65 refractive index) with a diameter of $0.45 \pm 0.01\,\mu$m and $1.25 \pm 0.05\,\mu$m were diluted in distilled water to a final concentration of a few particles/μl. A droplet (100 μl) of such solution was placed between a 150 μm-thick coverslip and a microscope slide, which were separated by a 100 μm-thick parafilm spacer and sealed with vacuum grease to prevent evaporation and contamination. Such sample cell was mounted on a closed-loop piezoelectric stage (Physik Instrumente PI-517.3CL), which allowed movements with nanometer resolution. The sample temperature was continuously monitored using a calibrated NTC thermistor positioned on the top surface of the microscope slide and remained constant within 0.2 degrees during each complete set of measurements.

A micro-sphere was trapped and positioned in the middle of the sample cell, i.e. far away from the glass surfaces to avoid hydrodynamic effects on the bead motion [10]. Its 3D position was monitored through the forward scattered light imaged on a a InGaAs Quadrant Photodiode (QPD, Hamamatsu G6849) at the back focal plane of the condenser lens [17], using a digital oscilloscope (Tektronix TDS5034B) for data-acquisition. The QPD-response was linear for displacements up to 300 nm (2 nm resolution, 250 kHz bandwidth). The conversion factor from voltage to distance was calibrated using the power spectral density method [18]. We excluded significant deviations from a harmonic trapping profile by verifying that the trapping potential could be fitted to such a profile in all the three directions.

Experimental results. – We performed the experiments using particles with diameter 0.45 μm and 1.25 μm. Similar particles are commonly employed in experiments that use optical traps [3]. The particle positions were acquired at 2.5 kHz, which is above the cutoff frequency of the particle motion in the optical trap and below the QPD bandwidth.

For a dataset of 2N+1 particle position – i.e. x_n, y_n and z_n for $n = -N, ..., -1, 0, 1, ..., N$ at times $t_n = 0.4 \cdot n$ ms – the experimental ACFs and DCCF are

$$\mathrm{ACF}_{\rho}^{(e)}(\tau = 0.4 \cdot m) = \sum_{n=-N}^{N} \rho_{m-n}\rho_n, \tag{9}$$

$$\mathrm{ACF}_{z}^{(e)}(\tau = 0.4 \cdot m) = \sum_{n=-N}^{N} z_{m-n}z_n, \tag{10}$$

and

$$\mathrm{DCCF}_{\rho,z}^{(e)}(\tau = 0.4 \cdot m) = \sum_{n=-N}^{N} \rho_{m-n}z_n - z_{m-n}\rho_n, \tag{11}$$

where $\rho_n = \sqrt{x_n^2 + y_n^2}$ and z_n are the time-series of the particle position in cylindrical coordinates.

For medium-high optical power at the sample (few tens of milliwatts) the $\mathrm{DCCF}_{\rho,z}^{(e)}(\tau) \cong 0$ within the experimental error. This is an evidence that the contribution of the non-conservative force-field component is effectively negligible, or at least undetectable for acquisition times up to several tens of minutes.

In order to have a non-vanishing DCCF the optical power at the sample needed to be reduced down to a few milliwatts. Furthermore, even under such low power a clearly non-vanishing DCCF was only obtained when the acquisition time was increased up to 400 s (i.e., $2N + 1 \approx 1 \times 10^6$ particle positions). It is an important remark the fact that, due to extremely low value of the rotational contribution to the total force-field, it is not immediately evident from the traces of the particle motion. Indeed the particle undergoes a random movement in the $\rho - z$ plane, where it is not possible to distinguish the presence of

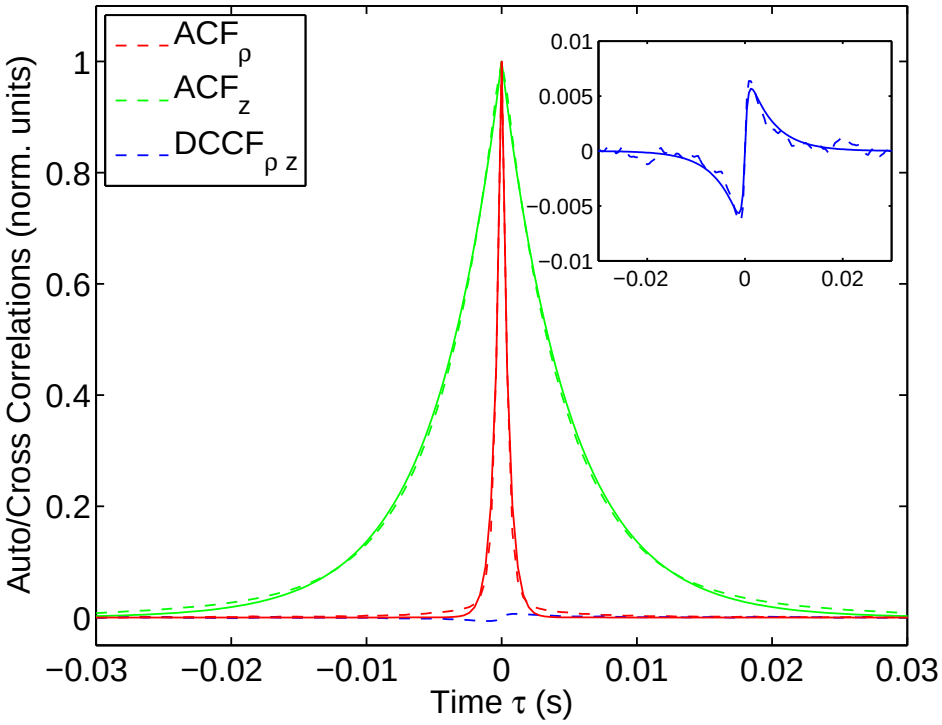

Fig. 3: Autocorrelation functions (ACFs) and difference of the cross-correlation function (DCCF) for a 0.45 μm colloidal particle optically trapped with a laser power of 6 mW at sample (first line of Tab. 1). Inset: close-up of the DCCF. Dashed lines represent experimental data, while solid lines are the curves obtained from the fit with Eq.(4), (5) and (6)

a rotational component without the aid of a statistical analysis such as the one we propose (see videos in the supplementary materials).

In Fig. 3 the ACFs and DCCF are presented for a 0.45 μm diameter particle held in an optical trap with an optical power at the sample of 6.0 mW (average of 10 400 s-datasets). A good agreement is found between the experimental and theoretical ACFs and DCCF. In particular, the experimental and theoretical DCCF are very similar over all the range of τ even though the fitting was performed only on the central slope. The amplitude of the DCCF is very small compared to the ACF one and the stiffness of the optical trap is quite low, only 5 $pN/\mu m$, compared to common experiments with optical tweezers.

In a very weak optical trap the particle can explore regions far away the trap-center. Thus the particle motion is more influenced by the non-conservative force. This means that the less power is used the more the DCCF amplitude is observed. This is shown in Figs. 4(A) where we can see the behavior of the DCCF for a 0.45 μm diameter particle while decreasing the optical power. The DCCF amplitude increases as the power decreases. Furthermore, the range over which the DCCF is not vanishing broadens. This translates into an increase of the rotational component relative weight for decreasing power as it is shown in Fig. 5(B).

In Fig. 4(B) we can see similar traces for a 1.25 μm. Again there is a good agreement between the experimental and theoretical DCCF over a wide range, even though the fitting was performed only on the central slope. Again the rotational component relative weight increases for decreasing power (Fig. 5(B)).

It is worth to be noted that if we compare the DCCF curves for the two diameters used

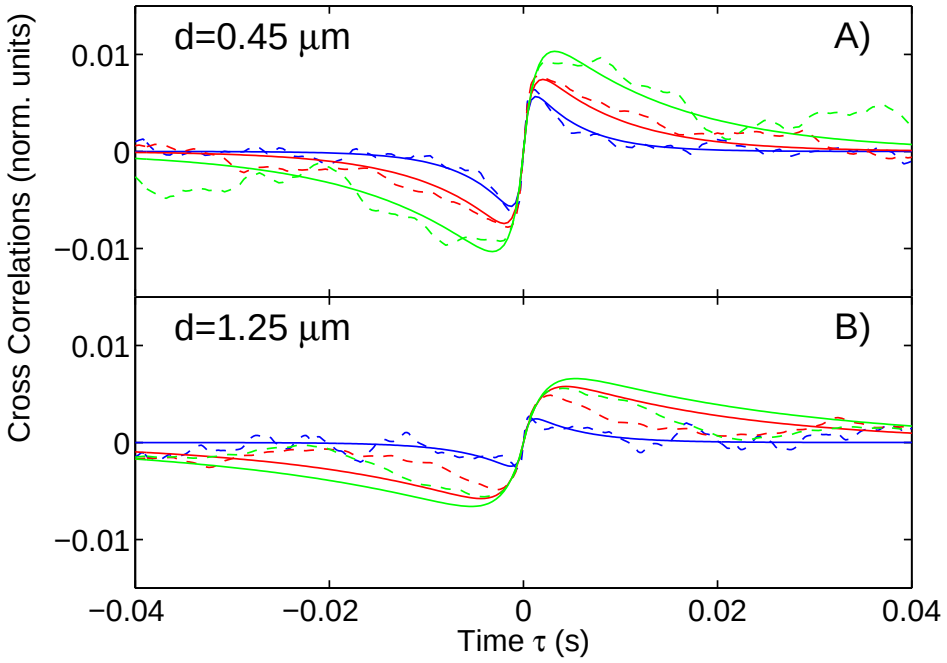

Fig. 4: Cross-correlation function for an optically trapped particle whose diameter is (A) 0.45 μm and (B) 1.25 μm. The powers used are listed in Tab. 1 and the color legend is: P(blue) > P(red) > P(green). Dashed lines represent experimental data, while solid lines are the curves obtaining from the fit

at comparable stiffness, i.e. $k_\rho = 2.9\ pN/\mu m$ for $d = 0.45\ \mu m$ and $k_\rho = 3.6\ pN/\mu m$ for $d = 1.25\ \mu m$ (second and last line of Tab. 1) we can observe a slightly larger amplitude for the smaller particle. Again this is a confirmation that the effect is due to the larger volume explored by the smaller particle with respect to the larger one.

In the Tab. 1 the numerical values for the studied cases are presented. The stiffness along the horizontal plane k_ρ is also shown in Fig. 5(A) where it can be appreciated the fact that it is linear with respect to the optical power. The ratio of the stiffness along z and ρ does not depend on the power used, while a clear increase of the rotational component ϵ is observed in both particle diameters used in this work. We notice that such values are similar to the ones reported in Ref. [13]. In their case the trap power is larger than the one used in the present experiment, but for the different setup the resulting stiffness is lower due to the fact that the particle size is larger (2 μm). Nevertheless the order of magnitude of the circulation they observed is in agreement with our data.

In particular the torque associated to the non-conservative component of the force-field is calculated according to Equation 7. The resulting values are extremely small (see Tab. 1), being actually orders of magnitude smaller than the ones previously reported, e.g., $4 \times 10^3 fN \cdot nm$ for the torque transfer from a Laguerre-Gaussian beam to a Brownian particle [5], $6 \times 10^3 fN \cdot nm$ for microscopic hydrodynamic flows [19], $1 \times 10^4 fN \cdot nm$ for DNA twist elasticity [20], $5 \times 10^6 fN \cdot nm$ for the movement of bacterial flagellar motors [21], $2 \times 10^4 fN \cdot nm$ for the transfer of orbital optical angular momentum [22], or $5 \times 10^5 fN \cdot nm$ for the transfer of spin optical angular momentum [23]. However, we must remark that in this letter we are focusing on the non-conservative forces that arise in a standard optical trap due to the fact that the trap is not perfectly harmonic in the vertical plane, while some of the previously mentioned examples, such as experiments with light beams that carry orbital

Table 1: The experimental parameters and the values obtained from the fit are reported here.

d	optical power	ρ-stiffness	$\frac{\text{z}-\text{stiffness}}{\rho-\text{stiffness}}$	rotational component	torque	circulation rate
$d\ (\mu m)$	$P\ (mW)$	$k_\rho\ (pN/\mu m)$	η	ϵ	$T\ (fN \cdot nm)$	$\Omega\ (Hz)$
0.45±0.01	6.0±0.2	5.0±0.1	16±1%	1.0±0.1 %	280±40	2.1±0.3
0.45±0.01	3.2±0.2	2.9±0.1	15±1%	1.7±0.2 %	490±60	2.1±0.3
0.45±0.01	1.0±0.2	1.68±0.07	16±1%	2.4±0.2 %	680±60	1.8±0.3
1.25±0.05	4.0±0.2	14.0±0.7	14±1%	0.7±0.1 %	210±30	1.4±0.2
1.25±0.05	1.4±0.2	4.4±0.2	13±1%	1.2±0.1 %	420±70	0.8±0.1
1.25±0.05	1.0±0.2	3.6±0.2	12±1%	3.8±0.3 %	1400±160	2.1±0.3

or spin angular momentum, refer to rather different situations in which the dominant effect is the presence of a non-conservative (or rotational) force field, which generates the particle movement.

Conclusions. – The $\text{DCCF}^{(e)}_{\rho,z}(\tau) \cong 0$ within the experimental error is a clear evidence that the contribution of the non-conservative force-field component is effectively negligible. This is actually true in most practical experimental situations. Typical optical tweezers experiments are performed with various tens of milliwatts of optical power at the sample

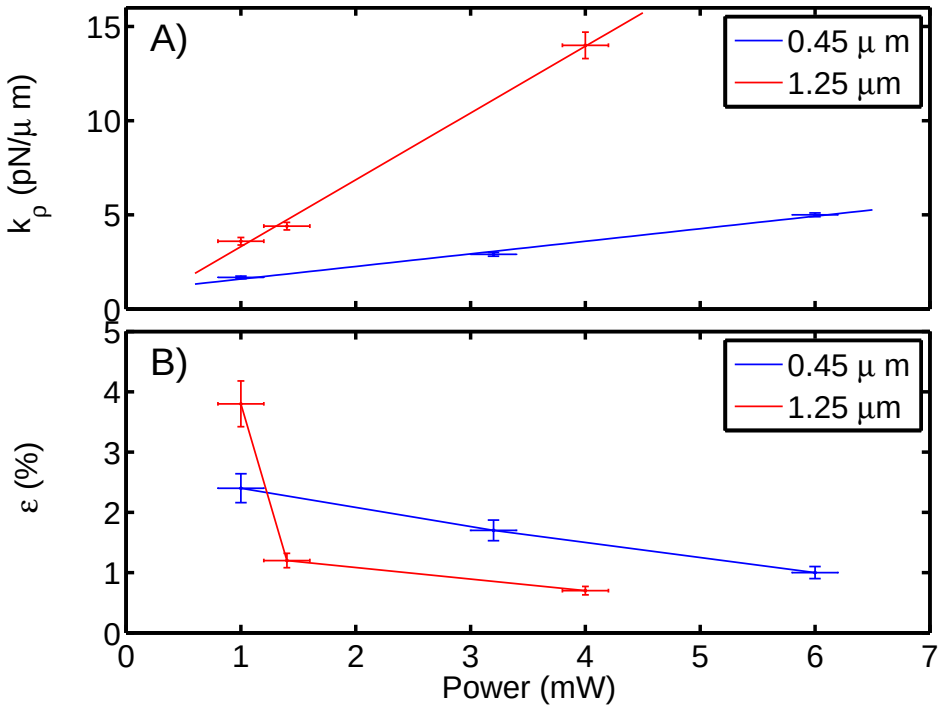

Fig. 5: (A) Behavior of the radial stiffness k_ρ as function of the laser power for the two kinds of particle used. The solid lines are the linear fits. (B) Value of the relative contribution of the non-conservative component ϵ as a function of the power used. Notice that it increases for lower powers.

and acquiring data for at most a few minutes [3]; however, we needed to decrease the optical power at the sample down to a range of a few milliwatts *and* to increase the acquisition time up to several minutes in order to see the signature of a non-conservative force-field component in the DCCF.

In particular, for medium-high laser powers (from a few tens of milliwatts at the sample onwards) the effect is undetectable even for long acquisition times – indeed, the value of ϵ steadily decreases as the laser power is increased (see Tab. 1 and Fig. 5(B)). This is due to the fact that the deviation from a conservative force-field is larger far from the trap center, which is explored more often in a weaker trap. Furthermore, this can also be seen in Figs. 6 and 7 of Ref. [12].

Therefore, we conclude that for the trapping regimes that are usually employed in experiments, the effect of the non-conservative force-field component are effectively negligible and do not affect the standard calibration procedure. Whenever a doubt is present, the extension to the standard optical tweezers calibration techniques we have proposed in this letter can be used to verify to what extend the assumption of a conservative force-field is fulfilled. In particular this technique might become increasingly useful as optical measurements of forces reach to ever smaller length and force scales, because these nonequilibrium effects will become increasingly noticeable.

* * *

The authors acknowledge fruitful discussions with Clemens Bechinger, Antonio Sasso and Dmitri Petrov. GR aknowledges CNISM for her research fellowship.

REFERENCES

[1] Ghislain L. P. and Webb W. W., *Opt. Lett.* , **18** (1993) 1678.
[2] Ghislain L. P., Switz N. A. and Webb W. W., *Rev. Sci. Instrumen.* , **65** (1994) 2762.
[3] Neumann K. C. and Block S. M., *Rev. Sci. Instrumen.* , **75** (2004) 2787.
[4] Rohrbach A., *Opt. Express* , **13** (2005) 9695.
[5] Volpe G. and Petrov D., *Phys. Rev. Lett.* , **97** (2006) 210603.
[6] Mazolli A., Neto P. A. M. and Nussenzveig H. M., *Proc. R. Soc. Lond. A* , **459** (2003) 3021.
[7] Harada Y. and Asakura T., *Opt. Commun.* , **76** (2005) 115105.
[8] Ashkin A., *Biophys. J.* , **61** (1992) 569.
[9] Visscher K., Gross S. P. and Block S. M., *IEEE J. Sel. Top. Quant. El.* , **2** (1996) 1066.
[10] Berg-Sørensen K. and Flyvbjerg H., *Rev. Sci. Instrumen.* , **75** (2004) 594.
[11] Volpe G., Volpe G. and Petrov D., *Phys. Rev. E* , **76** (2007) 061118.
[12] Merenda F., Boer G., Rohner J., Delacrétaz G. and R.-P-Salathé, *Opt. Express* , **14** (2006) 1685.
[13] Roichman Y., Sun B., Stolarski A. and Grier D. G., *Phys. Rev. Lett.* , **101** (2008) 128301.
[14] Purcell E. M., *Am. J. Phys.* , **45** (1977) 3.
[15] Happel J. and Brenner H., *Low Reynolds Number Hydrodynamics* (Spinger, New York) 1983.
[16] G.Pesce, A.Sasso and Fusco S., *Rev. Sci. Instrumen.* , **76** (2005) 115105.
[17] Gittes F. and Schmidt C., *Opt. Lett.* , **23** (1998) 7.
[18] Buosciolo A., Pesce G. and Sasso A., *Opt. Commun.* , **230** (2004) 357.
[19] Volpe G., Volpe G. and Petrov D., *Phys. Rev. E* , **77** (2008) 037301.
[20] Bryant Z., Stone M. D., Gore J., Smith S. B., Cozzarelli N. R. and Bustamante C., *Nature* , **424** (2003) 338.
[21] Berry R. M. and Berg H. C., *Proc. Natl. Acad. Sci.* , **94** (1997) 14433.
[22] Volke-Sepulveda K., Garcés-Chávez V., Chávez-Cerda S., Arlt J. and Dholakia K., *J. Opt. B* , **4** (2002) S82.
[23] Porta A. L. and Wang W. D., *Phys. Rev. Lett.* , **92** (2004) 190801.